Osteoporos Int (2012) 23:2313–2320
DOI 10.1007/s00198-011-1875-8

ORIGINAL ARTICLE

Three years of alendronate treatment does not continue to decrease microstructural stresses and strains associated with trabecular microdamage initiation beyond those at 1 year

J. O. Green · T. Diab · M. R. Allen · B. Vidakovic · D. B. Burr · R. E. Guldberg

Received: 31 May 2011 / Accepted: 27 October 2011 / Published online: 12 January 2012

Abstract
Summary The effects of a 3-year alendronate treatment on trabecular stresses/strains associated with microdamage initiation were investigated using finite element modeling (FEM). Severely damaged trabeculae in the low-dose treatment group were associated with increased stresses compared with the high-dose treatment group ($p=0.006$) and approached significance in the control group ($p=0.02$).
Introduction Alendronate, a commonly prescribed anti-remodeling agent, decreases fracture risk in the vertebrae, hip, and wrist of osteoporotic individuals. However, evaluation of microdamage accumulation in animal and human studies shows increased microdamage density relative to controls. Microstructural von Mises stresses associated with severe and linear damage have been found to decrease after 1 year of alendronate treatment. In the present study, stresses/strains associated with damage were assessed after 3 years of treatment to determine whether they continued to decrease with increased treatment duration.
Methods Microdamaged trabeculae visualized with fluorescent microscopy were associated with stresses and strains obtained using image-based FEM. Stresses/strains associated with severe, diffuse, and linearly damaged and undamaged trabeculae were compared among groups treated for 3 years with an osteoporotic treatment dose of alendronate, a Paget's disease treatment dose of alendronate, or saline control. Architectural characteristics and mineralization were also analyzed from three-dimensional microcomputed tomography reconstructed images.
Results Severely damaged trabeculae in the osteoporotic treatment dose group were associated with increased stress compared with the Paget's disease treatment dose group ($p=0.006$) and approached significance compared to the control group ($p=0.02$). Trabecular mineralization in severely damaged trabeculae of the low-dose treatment group was significantly greater compared to severely damaged trabeculae in the high-dose treatment and control group, suggesting that changes at the tissue level may play a role in these findings.
Conclusions Trabecular level stresses associated with microdamage do not continue to decrease with prolonged alendronate treatment. Changes in mineralization may account for these findings.

Keywords Bisphosphonate · Finite element modeling · Microcomputed tomography · Microdamage · Osteoporosis

J. O. Green · T. Diab · R. E. Guldberg (✉)
Parker H. Petit Institute for Bioengineering and Bioscience and George W. Woodruff School of Mechanical Engineering, Georgia Institute of Technology,
315 Ferst Drive,
Atlanta, GA 30332-0405, USA
e-mail: robert.guldberg@me.gatech.edu

J. O. Green
School of Medicine, Medical College of Georgia,
Augusta, GA, USA

M. R. Allen · D. B. Burr
Department of Anatomy and Cell Biology,
Indiana University School of Medicine,
Indianapolis, IN, USA

B. Vidakovic
Wallace H. Coulter Department of Biomedical Engineering,
Georgia Institute of Technology,
Atlanta, GA 30332, USA

D. B. Burr
Department of Biomedical Engineering,
Indiana University–Purdue University at Indianapolis,
Indianapolis, IN, USA

Introduction

Clinical studies have demonstrated bisphosphonates' efficacy at reducing osteoporotic fracture risk in areas with high levels of trabecular bone like the wrist, vertebral body, and proximal hip, primarily by reducing bone turnover to increasing bone mass [1–3]. However, bisphosphonate-associated gains in bone strength and stiffness at the apparent level come at the expense of changes in the mineral and organic phases that lead to a deterioration of the tissue level material properties. For instance, alendronate is associated with increased mean tissue age which contributes to improved bone strength and stiffness by increasing mineralization, but it also leads to an accumulation of advanced glycation end-products which can compromise bone toughness [4, 5]. These changes can increase the formation of microdamage and reductions in bone turnover can allow such damage to accumulate [6]. Indeed, increased microdamage density has been documented after 1 year of alendronate treatment in animal and human studies [6–8]. This is a concern because microdamage accumulation can impact tissue level material properties and may result in reduced tissue quality [9, 10]. Recent reports of the occurrence of atypical femoral fractures with long-term bisphosphonate use, although occurring in cortical rather than cancellous bone, nevertheless raise concerns about the effect of prolonged remodeling suppression on microdamage accumulation [11]. As alendronate is routinely used in the prevention and treatment of postmenopausal osteoporosis, long-term studies are needed that evaluate the impact of microdamage accumulation on trabecular bone mechanics.

From an engineering perspective, damage formation reflects the limit of bone to withstand forces from loading. Such limits can be quantified with stress and strain, used in previous studies to describe the micromechanical environment of trabecular bone [12, 13]. To describe the effects of mechanical loading, the magnitude of stress and strain can be computed using components of force/deformation based on loading along three principal axes (termed principal compressive stress or strain) or can include three-dimensional (3D) principal and shear components of forces/deformation (termed von Mises stress or strain). The von Mises yield criterion is particularly useful for describing the loading environment of trabeculae exhibiting severe or cross-hatched damage because this morphology suggests the contribution of shear forces in damage formation [13]. Principal compressive stresses/strains have also been used to characterize microstructural damage mechanics. As previous studies correlating these measures to microdamage incidents have failed to produce a dominant criterion, results from all of these measures are routinely investigated [14].

Image-based finite element modeling (FEM) is a powerful tool to evaluate the loading environment of a complex structure like trabecular bone. With this tool, a 3D representation of the structure is obtained using high-resolution computed tomography, and the contributions of trabecular geometry, material property, and spatial position are mathematically integrated to determine stresses and strains that describe the loading environment of a single trabecula. It is advantageous in small, complex systems because of the difficulty in obtaining individual trabecular stresses and strains from direct measurement. Therefore, use of this technique is ideal to evaluate changes in the mechanical adaptation of trabecular bone resulting from alendronate treatment over time.

In a recent study, increased microcrack density following 1 year of alendronate treatment correlated with decreased tissue level stresses associated with initiation of severe and linear damage [15]. It is unclear, however, whether such changes are sustained with continuation of treatment or whether there are adaptive responses. In the present study, stresses and strains associated with microdamage formation were obtained using image-based FEM of the distal femur from beagle dogs treated with 3 years of alendronate. By investigating the response of trabecular bone to damaging loads, microstructural changes that occur with prolonged treatment can be studied to determine factors which may contribute to the formation of microdamage. The goal of this study was to determine whether tissue level stresses and strains associated with damage initiation changed throughout the course of alendronate treatment. Based on observations of stabilized microdamage density with increased treatment duration, we hypothesized that damage initiation stresses and strains at 3 years' treatment will not be different from those at 1 year of treatment.

Methods

Animals

Detailed methods about the care and treatment regimen of animals whose tissues were used in this study have been published previously [16]. Briefly, 1-year-old skeletally mature beagle dogs were randomized into three groups and given either a saline solution control (n=4, 1 ml/kg/day) or alendronate every day at either a postmenopausal osteoporosis treatment dose (n=4, 0.2 mg/kg/day) or Paget's disease treatment dose (n=4, 1.0 mg/kg/day) for 3 years. All procedures were approved by the Indiana University School of Medicine Animal Care and Use Committee.

Trabecular bone core extraction and micro-CT imaging

The right distal femur from beagle dogs was secured using a vice such that the extraction angle was oriented parallel to

the principal material axis. Using a drill press with attached diamond-tipped core drill, 5-mm-diameter bone cores were extracted under constant irrigation with saline by coring through the condyle (#102055, Starlite Industries, USA). Cores comprised of trabecular bone from the metaphyseal region approximately 1 to 5 mm from the growth plate were sized to a final length of 18 mm with a diamond precision saw, and bone marrow was removed using a water pik (WP-72 W, WaterPik, USA). Stainless steel endcaps (5-mm depth) were glued with cyanoacrylate to each bone core end to prevent crushing and limit the effect of end artifacts on mechanical testing [17]. Cores were imaged with microcomputed tomography (micro-CT; μCT 40, Scanco Medical, Basserdorf, Switzerland) at a voxel resolution of 16 μm. Images were thresholded and evaluated to obtain values for bone volume fraction; trabecular thickness, number, and spacing; connectivity; structural model index (SMI); and degree of anisotropy. Mineralization was obtained from attenuation values of gray-scale micro-CT images based on hydroxyapatite (HA) calibration standards.

Fluorescent staining and mechanical testing

Trabecular bone cores were stained at atmospheric pressure and 4°C for 8 h in 0.02% alizarin complexone+10 μmol/l protease inhibitor (E-64, Sigma Chemical) then washed with distilled water for 1 h to fluorescently label preexisting damage, encompassing in vivo damage and damage occurring from the core extraction [18].

Cores were preconditioned for 3 cycles to 0.1% strain then loaded at a rate of 0.5% strain/second in displacement-controlled uniaxial compression to the yield strain, determined to be 1.2% in preliminary testing, and held for 3 h. The apparent strain was calculated using a gauge length of the exposed length of the bone measured with digital calipers plus half the length of each bone end embedded in endcaps [17]. During the test, cores were immersed in 0.9% physiological saline+10 μmol/l protease inhibitor.

After testing, the top endcap was removed with the diamond precision saw and cores were stained with 0.01% calcein at atmospheric pressure and 4°C for 8 h then washed with distilled water for 1 h to label test-induced damage [18]. Samples were held in 70% ethanol for 24 h then underwent a graded alcohol infiltration protocol to completely dehydrate the samples. Cores were embedded in methylmethacrylate; five slides of ~120-μm thickness were obtained beginning approximately 500 μm from the core edge and progressing inward toward the center of the core using a diamond precision saw. Sections were mounted onto slides in an orientation allowing for visual registration with the 3D micro-CT reconstructed image.

Histological evaluation

Microdamage was identified with fluorescent microscopy at 100× magnification based on the criteria that cracks are intermediate in size (20–150 μm; larger than canaliculi but smaller than vascular channels), have sharp borders, and have a focus plane demonstrating depth of field [6, 7]. A classification system published by Moore and Gibson [19] was modified to group damage into three broad morphological categories: severe, linear, and diffuse damage [15]. Severe damage was classified as microdamage consisting of either one primary crack with minor secondary cracks or cracks propagating through the thickness of the trabecula. Linear damage included both single and parallel cracks, and diffuse damage consisted of both cross-hatch damage equal in length and intensity (to distinguish it from severe damage) and damage with a large area of distribution. Areas of diffuse staining with no clearly defined cracks were not counted as microdamage. Investigators were blinded to the sample treatment group when conducting microdamage histological evaluations.

Finite element analysis and histological registration

The 3D reconstructed micro-CT image of each trabecular bone core was used to create high-resolution finite element models (FEM) of von Mises and principal compressive stress and strain distributions. Direct voxel conversion methods were used for mesh generation, and linear elastic, homogeneous, and isotropic material behavior were assumed [20]. Boundary conditions were applied which simulated uniaxial compressive loading to the yield strain. The tissue modulus was initially assigned to 10 GPa with a Poisson's ratio of 0.3.

Test-induced microdamaged and undamaged trabeculae identified and categorized histologically were visually registered to the 3D micro-CT reconstructed image, allowing for digital extraction of the trabeculae of interest from the lattice. A value for the mechanical parameter associated with damage type was obtained by averaging the value of all elements corresponding to the voxels along the extracted trabeculae. Only green fluorescing (test-induced) damage and undamaged trabeculae underwent this analysis (n=416 for control, n=391 for low dose, n=346 for high dose). Stress values were then scaled according to the ratio of the experimental Young's modulus calculated from the stress–strain curve during the mechanical test to the modulus obtained from the finite element solution using a back-calculation method [21]. A similar trabecular extraction method was used alongside detailed morphometric analysis of 3D reconstruction to determine architectural characteristics (SMI, thickness, orientation, and mineralization).

Statistics

All statistical tests were performed using MINITAB software (Minitab, Minitab Inc., USA). Parametric analyses were used for all comparisons after data met the requirement for normality. Differences in global architectural parameters between 3 years of treatment groups were determined with one-way analysis of variance (ANOVA) and Tukey's post hoc tests. Two-way ANOVA with Tukey's post hoc analysis was used to determine differences in global architectural parameters due to treatment group and treatment duration. Differences in crack density were determined with two-way ANOVA followed by Tukey's post hoc analysis for treatment group and damage type comparisons. All tests resulting in p-value less than 0.05 were considered statistically significant.

To determine differences in mechanical and architectural parameters of damaged and undamaged trabeculae by treatment group and microdamage category, two-way ANOVA with Tukey's post hoc analyses were performed. Three-way ANOVA with Tukey's post hoc comparisons were conducted to assess statistical significance of the mechanical or architectural parameters with respect to damage state, treatment effect, and treatment duration (using data from a similar 1-year study) [15]. A Bonferroni correction was applied to an alpha level of 0.05 for the multiple comparisons made for trabecular mechanical properties (von Mises stress, von Mises strain, principal compressive stress, and principal compressive strain). The correction was also applied for the multiple comparisons made in the trabecular architectural parameter analysis (trabecular thickness, SMI, orientation, and mineralization). This reduced the threshold for significance to $p \leq 0.0125$. All data are presented as mean ±standard error.

Results

Comparisons of global architectural properties across treatment groups showed no differences between groups following 3 years of treatment (Table 1). Between 1 and 3 years of treatment, mineralization increased in control (1 year: 1,011.9±6.2 mg HA/cm^3, 3 year: 1,081.5±15.0 mg HA/cm^3, $p<0.005$) and low-dose treatment groups (1 year: 1,040.3±6.1 mg HA/cm^3, 3 year: 1,091.1±12.6 mg HA/cm^3, $p<0.03$). Increased mineralization in the high-dose treatment groups was not significant (1 year: 1,040.3±0.9 mg HA/cm^3, 3 year: 1,077.3±30.0 mg HA/cm^3).

The trabecular von Mises stress of each damage state was compared within treatment and control groups. As might be expected, severely damaged trabeculae were under greater von Mises stress than all other damage types within each treatment and control group (Fig. 1, $p<0.001$). Also, diffusely damaged trabeculae demonstrated greater von Mises stresses compared to undamaged trabeculae in both the low-dose treatment group and controls ($p<0.001$).

When von Mises stresses associated with damage were compared between groups, treatment differences emerged. With the low-dose alendronate treatment, severely damaged trabeculae were associated with greater von Mises stresses than those in the high-dose treatment ($p=0.006$) and control group (Fig. 1, $p=0.02$ approached significance). Similar results were observed using an alternate stress measure, principal compressive stress, except that stress comparisons of severely damaged trabeculae between treatment and control groups did not achieve significance ($p=0.02$ between low-dose and high-dose treatment; $p=0.04$ between low-dose treatment and control). Interestingly, von Mises stresses associated with severe damage increased from 1 to 3 years in the low-dose treatment group ($p<0.001$). No similar differences using principal compressive stresses were observed.

Further characterization of the trabecular mechanical response to loading was achieved by evaluating strain differences (both von Mises and principal compressive) among treatment and control groups. Similar to the von Mises stress results, severely damaged trabeculae were under significantly greater strain than all other damage types in the control and low-dose treatment group (Fig. 2, $p<0.001$), and all but diffusely damaged trabeculae in the high-dose treatment group ($p<0.001$). Von Mises strains were not different between treatment groups. However, principal compressive

Table 1 Global architectural characteristics by treatment group

Parameter	Control	0.2 mg/kg/day	1.0 mg/kg/day	p-Value
Bone volume fraction (BV/TV)	0.22±0.07	0.19±0.03	0.20±0.04	0.74
Connectivity density (mm^{-3})	20.8±1.0	23.8±2.6	22.5±2.3	0.19
Structural model index (SMI)	1.1±0.7	1.2±0.2	0.95±0.58	0.75
Trabecular number (mm^{-1})	2.2±0.1	2.2±0.1	2.2±0.1	0.94
Trabecular thickness (μm)	115.8±17.5	104.8±17.8	98.6±8.6	0.31
Degree of anisotropy (DA)	1.49±0.20	1.47±0.04	1.51±0.12	0.90
Mineralization (mg HA/cm^3)	1,081.5±15.0	1,091.1±12.6	1,077.3±30.0	0.64
Tissue modulus (GPa)	11.5±2.7	13.6±2.8	12.2±2.8	0.59

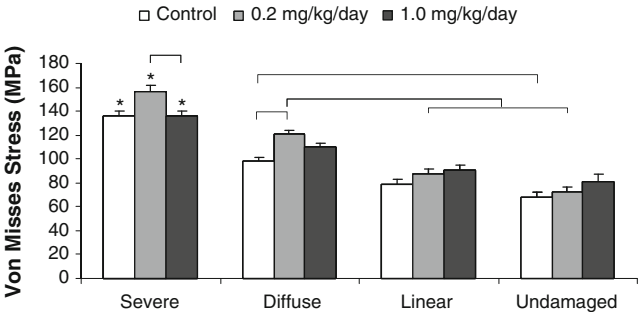

Fig. 1 Von Mises stress values by damage type and treatment group. Significantly increased stresses in severely damaged trabeculae relative to all other damage types were observed in each treatment group (*). Stresses were also increased in severely damaged trabeculae in the low-dose treatment group compared with those in the high-dose treatment group, and approached significance compared to the control group. In the low-dose treatment group, stresses were increased in diffusely damaged trabeculae relative to controls. Bars represent significant differences, $p<0.012$; mean±SEM plotted

strain comparisons showed significant increases among severely damaged trabeculae treated with low-dose alendronate compared with the high-dose treatment group ($p<0.01$). No differences in either strain measure were seen between 1 and 3 years of treatment.

Because trabecular architecture can influence stresses and strains, all trabeculae were described by their SMI value, thickness, orientation, and mineralization. When SMI, which describes whether a trabecula is more plate-like (lower number) or rod-like (higher number), was evaluated, diffusely damaged trabeculae exhibited more plate-like architecture compared with the more rod-like severe and undamaged trabeculae in treatment and control groups (Fig. 3a, $p<0.01$). A comparison of trabecular thickness showed that thinner trabeculae were more likely to sustain severe damage regardless of treatment group (Fig. 3b, $p<0.01$). No association with trabecular orientation was noted

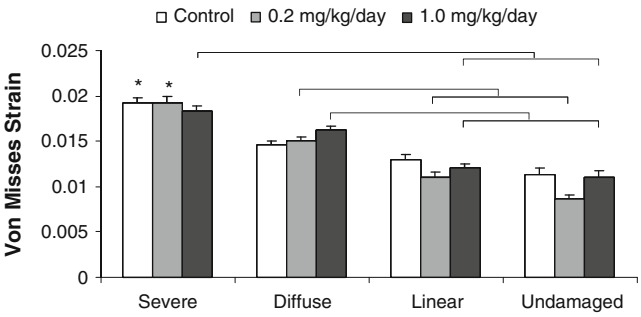

Fig. 2 Von Mises strain values by damage morphology and treatment group. Significantly increased trabecular strains in severely damaged trabeculae were seen compared with all other damage types in the control and low-dose treatment group (*) and in linearly damaged and undamaged trabeculae in the high-dose treatment group. Diffusely damaged trabeculae were also under increased strain compared with linear and undamaged trabeculae in both treated groups. *Bars* indicate significant differences, $p<0.012$; mean±SEM plotted

in any treatment or control group (Fig. 3c). When trabecular mineralization was evaluated, however, mineralization of severely damaged trabeculae was greater in the low-dose treatment group compared with both controls and high-dose treatment group; in controls, severely damaged trabeculae were less mineralized than undamaged (Fig. 3d).

Finally, microdamage incidents were counted and compared between treatment and control groups. Preexisting (alizarin-labeled) damage was largely of a linear morphology, with an increased linear damage density in the high-dose treatment group (1.03±0.14 incidents/mm^2) compared with low-dose (0.45±0.05 incidents/mm^2) and control group (0.47±0.08 incidents/mm^2, $p<0.01$). However, there was more test-induced (calcein-labeled) damage than preexisting damage in all treatment and control groups (Fig. 4, $p<0.05$). Damage exhibiting both the alizarin and calcein stain was totaled separately, and no differences were found between treatment or control groups. Damage totals (the sum of preexisting, test-induced, and dual-stained damage) were not significantly different between treatment or control groups. Also, damage totals were not significantly different between 1 and 3 years of treatment.

Discussion

In this study, the effects of 3 years of daily alendronate treatment on trabecular stresses and strains associated with microdamage initiation were investigated using image-based FEM. Stresses obtained from FEM were linearly scaled to reflect specimen-specific differences in stiffness calculated from the linear elastic region of the apparent level stress–strain curve [21]. This method ensures that average tissue level stresses between groups are similar despite differences in bone volume fraction and mineralization which influence the mechanical strength and maximum applied load. It was found that severely damaged trabeculae in the low-dose alendronate treatment group were associated with increased stresses compared with the high-dose treatment group ($p=0.006$) and approached significance in the control group ($p=0.02$). This finding reverses a trend observed in a similar study conducted after 1 year of treatment at the same doses, where von Mises stresses of severely and linearly damaged trabeculae were significantly decreased in alendronate-treated groups compared with controls [15]. These results suggest that while alendronate may reduce the stresses associated damage formation after 1 year of treatment, by 3 years of treatment the tissue level properties have stabilized relative to controls.

Overall, trabecular level stresses and strains remained relatively consistent between 1 and 3 years in all treatment and control groups. An increase in von Mises stresses associated with severe damage in the low-dose treatment group

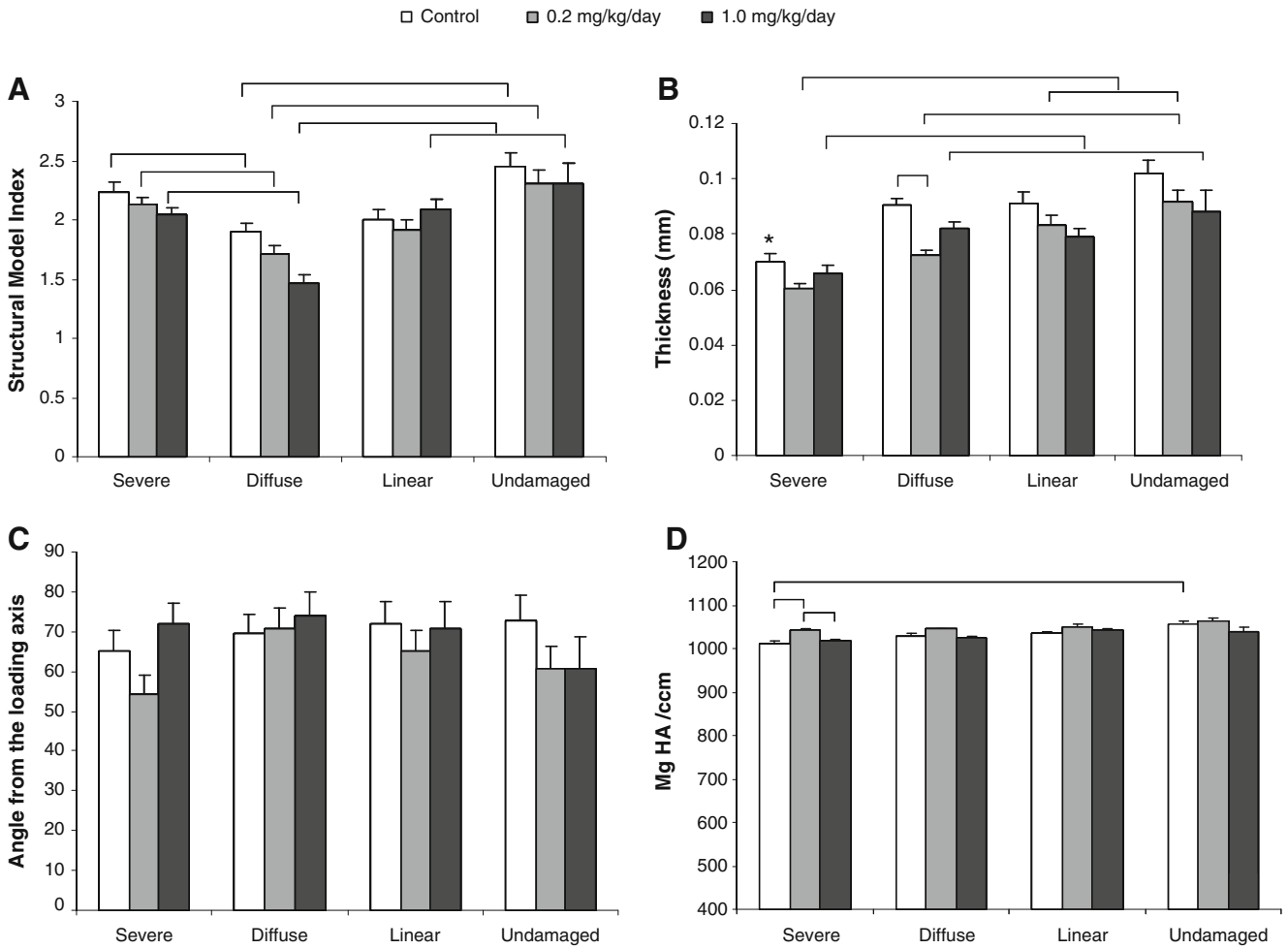

Fig. 3 Architectural characteristics of trabeculae by damage type and treatment group. **a** Characterization of the SMI of damaged trabeculae showed rod-like architecture of severe and undamaged trabeculae relative to diffusely damaged trabeculae in all treatment groups. **b** Severely damaged trabeculae were thinner than undamaged trabeculae in all treatment groups. Severely damaged trabeculae were thinner than all other damage types in the control group (*). **c** Evaluation of the trabecular orientation relative to the loading axis did not show differences in the formation of damage of different morphologies. **d** Severely damaged trabeculae in the low-dose treatment group were significantly more mineralized than severely damaged trabeculae in the high-dose and control groups. $p<0.012$, *bars* represent significant differences. Mean±SEM plotted

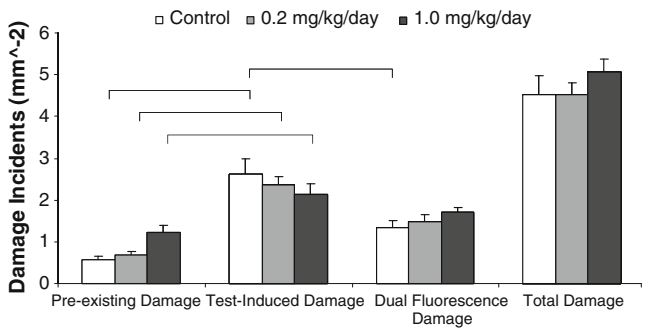

Fig. 4 Damage quantification totals by treatment group. There were significantly increased test-induced damage incidents compared with preexisting damage incidents in each treatment group. Also, there was more test-induced damage than damage demonstrating dual fluorescence in the control group. *Bars* indicate significant differences, $p<0.05$; mean±SEM is plotted

was the only treatment durational difference noted. Thus, the extension of alendronate treatment to 3 years does not continue to decrease damage initiation stresses relative to controls, as seen after 1 year of treatment. Rather, the susceptibility of trabecular bone to microdamage formation appears to stabilize, and microdamage quantification data reported in this study and others corroborate this conclusion [16]. This finding is important toward understanding the consequences of long-term bone turnover suppression on trabecular bone mechanics.

One possible explanation for the stress findings is that microstructural changes occurring during treatment modulate the mechanical loading environment to limit further damage formation. Because bone turnover is suppressed with alendronate, secondary mineralization is more complete in bone multicellular units and may provide additional

strength against damaging forces [22]. In particular, the changes in material strength associated with the increased mineralization quantified in this study may increase the ability of the structure to withstand higher stresses/strains without damaging. Lending support to this theory, we observed a significant increase in the mineralization of severely damaged trabeculae from the low-dose treatment group compared with those in the high-dose treatment group and controls (Fig. 3d). Furthermore, the mineral density was significantly increased in the severely damaged trabeculae at 3-year low-dose alendronate as compared to values after 1 year of treatment at the same dose ($p<0.001$) [15]. Though our finite element models were homogenous and did not account for local stiffness heterogeneity due to mineralization in stress calculations, values for microstructural stresses were scaled according to the stiffness at the apparent level, resulting in an 11% increase in the back-calculated tissue modulus between 1 and 3 years in the low-dose treatment group. We speculate that these changes in the mineralization profile at the microstructural level contribute to increased resistance to damage initiation.

Another proposed mechanism which explains why microdamage density does not continue to increase with prolonged alendronate treatment is that a new equilibrium for remodeling is established which is able to control further damage formation. Though this study did not explicitly measure and compare bone turnover rate changes across 1 and 3 years of treatment, one effect of a new, prolonged equilibrium bone turnover rate with bisphosphonate treatment would be to allow for an increased degree of mineralization, thus serving to stiffen the material and increase stresses associated with damage. It is very likely that both mechanisms act concurrently to limit damage formation when treatment effects on bone microstructure are fully realized.

Finally, architectural characteristics of trabeculae were analyzed for changes linked with stress/strain findings. Evaluation of the architectural characteristics within damage morphological groups revealed few differences between treatment and control groups and few changes from 1 to 3 years. Decreased trabecular thickness and rod-like geometry were associated with severe damage formation in this study, and the observation has been made by others in different populations [23, 24]. This morphology is typical of trabeculae in osteoporotic or older individuals and suggests the potential for greater damage to accrue in these populations based on considerations of trabecular architecture alone, even without bisphosphonate treatment. However, it is unlikely that changes in individual trabecular architecture accounted for stress/strain changes observed in this study.

We hesitate to conclude that, overall, bone quality is improved with prolonged alendronate treatment, because other studies have documented decreased toughness in alendronate-treated bone but did not attribute such findings to microdamage formation [16, 25]. Previous work in these animals has documented that remodeling suppression with bisphosphonates is associated with significant increases in both enzymatic and nonenzymatic collagen cross-links, the latter being correlated with reduced bone quality [5, 26]. The current study does not take into account any changes to collagen. Thus, the bone quality improvements between 1 and 3 years of alendronate treatment are specific to those that lead to the formation of severe microcrack formation in trabecular bone.

A number of limitations must be considered when placing the results of this study in the context of fracture risk with prolonged alendronate treatment. The use of intact (nonovariectomized), relatively young beagle dogs limits the translation of this study's findings to osteoporotic human populations, and the small number of samples in each group may not capture the full variability of trabecular bone architecture in the population. In particular, we did not observe an expected increase in the bone volume fraction of alendronate-treated trabecular bone, and this finding is likely related to the small sample size. Additionally, while assumptions of linear elasticity, isotropy, and homogeneity at the microstructural level provide a good estimate of tissue level mechanical properties, they are not completely accurate in describing tissue level trabecular behavior, particularly when used to understand evolving properties in the face of microdamage progression. For this reason, it should be understood that stress/strain calculations refer only to predictions from the undamaged state and do not account for changes which may occur once the damage initiation process has begun. However, this study illuminates the microstructural mechanics associated with microdamage formation and sheds some light on the effect of alendronate administration on those mechanisms.

In this study, tissue level stresses and strains from alendronate-treated trabecular bone were computed with FEM, registered with histological observations of microdamage incidents, and compared to stress/strain levels in control groups and also with results from a similar study conducted after 1 year of treatment. We conclude that changes in damage initiation stresses/strains occur early in treatment (within the first year) and do not continue to deteriorate with alendronate treatment up to 3 years. We speculate that increases in trabecular mineralization may account for these findings.

Acknowledgements This study was supported by NIH grants 5R01AG027249, 5R01AR047838, and 5T32AR007581. Merck kindly provided the alendronate. The micro-CT system was provided by an NSF Major Research Instrumentation Award (9977551).

Conflicts of interest Dr. Burr receives grant/research support from Eli Lilly, Procter and Gamble Pharmaceuticals, The Alliance for Better Bone Health, Pfizer, and NephroGenex. He is a consultant/scientific advisor for Eli Lilly, Procter and Gamble Pharmaceuticals, Amgen, and PharmaLegacy. He is a speaker for Amgen and Eli Lilly. The other authors have no conflicts of interest.

References

1. Black DM, Cummings SR, Karpf DB, Cauley JA, Thompson DE, Nevitt MC, Bauer DC, Genant HK, Haskell WL, Marcus R, Ott SM, Torner JC, Quandt SA, Reiss TF, Ensrud KE (1996) Randomised trial of effect of alendronate on risk of fracture in women with existing vertebral fractures. Fracture intervention trial research group. Lancet 348(9041):1535–1541
2. Black DM, Thompson DE, Bauer DC, Ensrud K, Musliner T, Hochberg MC, Nevitt MC, Suryawanshi S, Cummings SR (2000) Fracture risk reduction with alendronate in women with osteoporosis: the fracture intervention trial. FIT research group. J Clin Endocrinol Metab 85(11):4118–4124
3. Rodan GA, Reszka AA (2002) Bisphosphonate mechanism of action. Curr Mol Med 2(6):571–577
4. Allen MR, Burr DB (2007) Mineralization, microdamage, and matrix: how bisphosphonates influence material properties of bone. Bone Key Osteovision 4(2):49–60
5. Tang SY, Allen MR, Phipps R, Burr DB, Vashishth D (2009) Changes in non-enzymatic glycation and its association with altered mechanical properties following 1-year treatment with risedronate or alendronate. Osteoporos Int 20(6):887–894
6. Allen MR, Iwata K, Phipps R, Burr DB (2006) Alterations in canine vertebral bone turnover, microdamage accumulation, and biomechanical properties following 1-year treatment with clinical treatment doses of risedronate or alendronate. Bone 39(4):872–879
7. Stepan JJ, Burr DB, Pavo I, Sipos A, Michalska D, Li J, Fahrleitner-Pammer A, Petto H, Westmore M, Michalsky D, Sato M, Dobnig H (2007) Low bone mineral density is associated with bone microdamage accumulation in postmenopausal women with osteoporosis. Bone 41(3):378–385
8. Mashiba T, Hirano T, Turner CH, Forwood MR, Johnston CC, Burr DB (2000) Suppressed bone turnover by bisphosphonates increases microdamage accumulation and reduces some biomechanical properties in dog rib. J Bone Miner Res 15(4):613–620
9. Schaffler MB, Radin EL, Burr DB (1989) Mechanical and morphological effects of strain rate on fatigue of compact bone. Bone 10(3):207–214
10. Ruppel ME, Burr DB, Miller LM (2006) Chemical makeup of microdamaged bone differs from undamaged bone. Bone 39 (2):318–324
11. Shane E, Burr D, Ebeling PR, Abrahamsen B, Adler RA, Brown TD, Cheung AM, Cosman F, Curtis JR, Dell R, Dempster D, Einhorn TA, Genant HK, Geusens P, Klaushofer K, Koval K, Lane JM, McKiernan F, McKinney R, Ng A, Nieves J, O'Keefe R, Papapoulos S, Sen HT, van der Meulen MC, Weinstein RS, Whyte M (2010) American Society for Bone and Mineral Research. J Bone Miner Res 25(11):2267–2294
12. Yeni YN, Zelman EA, Divine GW, Kim DG, Fyhrie DP (2008) Trabecular shear stress amplification and variability in human vertebral cancellous bone: relationship with age, gender, spine level and trabecular architecture. Bone 42(3):591–596
13. Fyhrie DP, Hoshaw SJ, Hamid MS, Hou FJ (2000) Shear stress distribution in the trabeculae of human vertebral bone. Ann Biomed Eng 28(10):1194–1199
14. Nagaraja S, Couse TL, Guldberg RE (2005) Trabecular bone microdamage and microstructural stresses under uniaxial compression. J Biomech 38(4):707–716
15. O'Neal JM, Diab T, Allen MR, Vidakovic B, Burr DB, Guldberg RE (2010) One year of alendronate treatment lowers microstructural stresses associated with trabecular microdamage initiation. Bone 47(2):241–247
16. Allen MR, Burr DB (2007) Three years of alendronate treatment results in similar levels of vertebral microdamage as after one year of treatment. J Bone Miner Res 22(11):1759–1765
17. Keaveny TM, Pinilla TP, Crawford RP, Kopperdahl DL, Lou A (1997) Systematic and random errors in compression testing of trabecular bone. J Orthop Res 15(1):101–110
18. O'Brien FJ, Taylor D, Lee TC (2002) An improved labelling technique for monitoring microcrack growth in compact bone. J Biomech 35(4):523–526
19. Moore ATL, Gibson LJ (2002) Microdamage accumulation in bovine trabecular bone in uniaxial compression. J Biomech Eng 124(1):63–71
20. van Rietbergen B, Weinans H, Huiskes R (1996) Computational strategies for iterative solutions of large FEM applications employing voxel data. Int J Numer Methods Eng 39:2743–2767
21. van Rietbergen B, Weinans H (1995) Huiskes R, Odgaard A, A new method to determine trabecular bone elastic properties and loading using micromechanical finite-element models. J Biomech 28(1):69–81
22. Boivin G, Meunier PJ (2002) Effects of bisphosphonates on matrix mineralization. J Musculoskelet Neuronal Interact 2(6):538–543
23. Shi X, Liu XS, Wang X, Guo XE, Niebur GL (2010) Effects of trabecular type and orientation on microdamage susceptibility in trabecular bone. Bone 46(5):1260–1266
24. Arlot ME, Burt-Pichat B, Roux J-P, Vashishth D, Bouxsein ML, Delmas PD (2008) Microarchitecture influences microdamage accumulation in human vertebral trabecular bone. J Bone Miner Res 23(10):1613–1618
25. Allen MR, Reinwald S, Burr DB (2008) Alendronate reduces bone toughness of ribs without significantly increasing microdamage accumulation in dogs following 3 years of daily treatment. Calcif Tissue Int 82(5):354–360
26. Allen MR, Gineyts E, Leeming DJ, Burr DB, Delmas PD (2008) Bisphosphonates alter trabecular bone collagen cross-linking and isomerization in beagle dog vertebra. Osteoporos Int 19(3):329–337